APPLIED AND ENVIRONMENTAL MICROBIOLOGY, Mar. 1998, p. 982–991 Vol. 64, No. 3
0099-2240/98/$04.00+0

Fermentation, Purification, and Characterization of Protective Antigen from a Recombinant, Avirulent Strain of *Bacillus anthracis*

J. W. FARCHAUS,* W. J. RIBOT, S. JENDREK, AND S. F. LITTLE

Bacteriology Division, U.S. Army Medical Research Institute of Infectious Diseases, Fort Detrick, Frederick, Maryland 21702-5011

Received 22 October 1997/Accepted 23 December 1997

***Bacillus anthracis*, the etiologic agent for anthrax, produces two bipartite, AB-type exotoxins, edema toxin and lethal toxin. The B subunit of both exotoxins is an M_r 83,000 protein termed protective antigen (PA). The human anthrax vaccine currently licensed for use in the United States consists primarily of this protein adsorbed onto aluminum oxyhydroxide. This report describes the production of PA from a recombinant, asporogenic, nontoxigenic, and nonencapsulated host strain of *B. anthracis* and the subsequent purification and characterization of the protein product. Fermentation in a high-tryptone, high-yeast-extract medium under nonlimiting aeration produced 20 to 30 mg of secreted PA per liter. Secreted protease activity under these fermentation conditions was low and was inhibited more than 95% by the addition of EDTA. A purity of 88 to 93% was achieved for PA by diafiltration and anion-exchange chromatography, while greater than 95% final purity was achieved with an additional hydrophobic interaction chromatography step. The purity of the PA product was characterized by reversed-phase high-pressure liquid chromatography, sodium dodecyl sulfate (SDS)-capillary electrophoresis, capillary isoelectric focusing, native gel electrophoresis, and SDS-polyacrylamide gel electrophoresis. The biological activity of the PA, when combined with excess lethal factor in the macrophage cell lysis assay, was comparable to previously reported values.**

The gram-positive organism *Bacillus anthracis*, the etiologic agent of anthrax, is the only member of the genus *Bacillus* capable of causing epidemic disease in humans and other mammals. *B. anthracis* grows in long chains and is nonmotile; virulent strains harbor two endogenous plasmids, pXO1 (29, 43) and pXO2 (10, 46), which code for the major known virulence factors of this organism. Plasmid pXO2 harbors the genes responsible for the synthesis of the glutamyl polypeptide capsule, which gives the strains their characteristic mucoid appearance in the presence of bicarbonate (10, 24, 25). Plasmid pXO1 harbors the structural genes for toxin production and regulation (30, 39–42, 48). Toxigenic *B. anthracis* strains secrete two bipartite exotoxins, lethal toxin and edema toxin. The secreted M_r 83,000 protein, known as protective antigen (PA), serves as the B component of both toxins (20). It binds to an unidentified receptor on the cell surface, where it is cleaved by cellular protease(s) to an M_r 63,000 form that exposes the binding site for the A components lethal factor (LF) and edema factor (EF), which bind competitively (4, 9, 17).

It was discovered during the late 1800s and early 1900s that cultures of virulent *B. anthracis* could be attenuated by growth at 42 to 43°C. The attenuation observed with such Pasteur-type vaccine strains resulted from the loss of plasmid pXO1. Fully virulent $pXO2^+$ $pXO1^+$ strains were thus attenuated by conversion to the $pXO2^+$ $pXO1^-$ genotype. Other attenuated strains, such as the Sterne strain, spontaneously lost pXO2 while retaining pXO1. Culturing the Sterne strain at 42°C resulted in the loss of pXO1 and produced the avirulent $pXO1^-$ $pXO2^-$ strain referred to as ΔSterne-1 (11).

The currently licensed human vaccine is produced by growing the $pXO1^+$ $pXO2^-$ V770-NP1-R strain of *B. anthracis* in minimal medium in the presence of bicarbonate under microaerophilic conditions and adsorbing the sterile filtered culture supernatant to aluminum oxyhydroxide adjuvant (36, 37). The protective component of the vaccine appears to be PA. Although the vaccine has proven efficacious (7, 13, 14, 37), the current vaccine strain has several limitations, including a sporogenic and fully toxigenic genotype. Production of vaccine from this strain results in lot-to-lot variability due to inconsistent PA production levels, inclusion of undefined PA proteolytic degradation products, and inclusion of other bacterial products including LF and EF (31).

To eliminate these limitations, an avirulent, nontoxigenic strain, ΔSterne-1, was selected as a host for PA expression. The recombinant plasmid pPA102 was created by subcloning a 6-kb *Bam*HI fragment harboring the PA structural gene and flanking sequence originally cloned from the endogenous *B. anthracis* plasmid pXO1 (15). The 6-kb fragment was inserted into the gram-positive vector pUB110 and transformed into *B. subtilis* 1S53, and PA-positive transformants were selected (15). Subsequent characterization of the *B. subtilis* transformants revealed that spontaneous deletions had occurred, resulting in the loss of substantial portions of the original 6-kb insert, including the bicarbonate regulation (42) of PA production. A stable kanamycin-resistant, PA-positive version of the plasmid was isolated and termed pPA102 (15). This plasmid was electrotransformed into *B. anthracis* ΔSterne-1 to specifically restore constitutive PA production (12). Subsequently, an asporogenic variant was selected and characterized (49). We describe here the fermentation, purification, and characterization of recombinant PA produced from ΔSterne-1(pPA102)CR4.

MATERIALS AND METHODS

Bacterial strains and culture conditions. The *B. anthracis* $pXO1^-$ $pXO2^-$ ΔSterne-1 strain used in this study (11) was electrotransformed with pPA102

* Corresponding author. Mailing address: Bacteriology Division, USAMRIID, 1425 Porter St., Fort Detrick, MD 21702-5011. Phone: (301) 619-4931. Fax: (301) 619-2152. E-mail: dr._joseph_farchaus @ftdetrck-ccmail.army.mil.

(15), and transformants displaying a stable PA-positive, kanamycin-resistant, LF-negative, EF-negative, and capsule-negative phenotype were selected (12). An asporogenic variant, ΔSterne-1(pPA102)CR4, was then selected and provided by Worsham and Sowers (49). The working stock was stored at −70°C in 50% (vol/vol) glycerol.

ΔSterne-1(pPA102)CR4 was grown at 37°C on solid medium consisting of 33 g of tryptone (Difco, Detroit, Mich.), 20 g of yeast extract (Difco), 2 g of L-histidine, 8 g of Na_2HPO_4, 7.4 g of NaCl, 4 g of KH_2PO_4, 15 g of Bacto Agar (Difco), and 40 mg of kanamycin sulfate per liter and adjusted to pH 7.4 with NaOH. Liquid cultures were grown in the same medium without kanamycin or Bacto Agar. Fermentation cultures contained 2 ml of antifoam KFO673 (Kabo Chemical Co., Jackson Hole, Wyo.), which was added to the complete medium before sterilization. A minimum volume of a sterile 1:4 dilution of KFO673 in Milli-Q (MQ) (Millipore Corp., Marlborough, Mass.) water was added as necessary during the fermentation. Unless otherwise specified, chemicals were obtained from Sigma (St. Louis, Mo.)

Fermentation conditions. The fermentations were performed with a Micros I top-drive fermentor (New Brunswick Scientific, New Brunswick, N.J.) with a 20-liter-working-volume 316-L stainless steel vessel equipped with two Rushton impellers whose diameter was equal to one-third the vessel diameter. The lower impeller was positioned on the drive shaft at a distance equal to the impeller diameter from the bottom of vessel, while the remaining impeller was positioned 1.5 times the impeller diameter above the lower impeller. The fermentor was also equipped with an ML4100 process controller, a two-gas mixer, and Advanced Fermentation software (New Brunswick Scientific). The vessel and medium were sterilized by exposure to 121°C for 15 min. The short sterilization cycle was required to minimize Millard-type and other medium degradation reactions. The total elapsed time at temperatures in excess of 37°C was less than 45 min. Subsequent testing revealed that medium sterility was maintained for more than 48 h under growth conditions.

The polarographic dissolved oxygen (DO_2) probe (Ingold, Wilmington, Pa.) was calibrated after 16 h of polarization by setting the DO_2 zero value to 0 nA with a DO_2/pH simulator (Valley Instrument Co., Exton, Pa.). The 100% value was set to the oxygen tension at 37°C in the medium after aeration with air (1 vol/vol/min) at an agitation rate of 250 rpm. The gel-filled pH probe (Ingold) was calibrated between pH 7 and 10 before sterilization by using standard buffers and the method described by the manufacturer.

A vial of ΔSterne-1(pPA102)CR4 working stock was thawed at the start of each 20-liter fermentation, and a 100-μl aliquot was immediately streaked onto solid medium in a plate and incubated for 7 to 12 h at 37°C. A 200-ml volume of liquid medium in a 1-liter baffled Erlenmeyer flask (Bellco, Vineland, N.J.) was inoculated with the growth from the plate and incubated at 37°C with shaking at 150 rpm for 6 to 7 h. The entire 200-ml subculture was then added to 800 ml of medium in a 4-liter baffled Erlenmeyer flask. This seed culture was incubated at 37°C with shaking at 150 rpm for an additional 6 to 7 h until a maximum optical density at 600 nm (OD_{600}) between 1.5 and 3.5 was attained. The 5% (vol/vol) seed culture volume was transferred aseptically to the 20-liter fermentor. The initial OD_{600} was recorded, and a sample of the inoculum was streaked on sheep blood agar plates and incubated overnight at 37°C to verify inoculum purity.

DO_2 values were maintained at 75% of saturation during the fermentations by increasing the agitation from the initial 250 rpm to a maximum of 500 rpm. Once the rpm maximum was achieved, the two-gas mixer supplemented the process air with pure oxygen while holding the sparging rate constant at 1 vol/vol/min. The mixture rate and percentages of air and pure oxygen were controlled by the two-gas mixer, with the relative proportions of air and oxygen being governed by an AFS (New Brunswick) algorithm which increased or decreased the percentage of oxygen in response to the current measured DO_2 value during the fermentation. Both gases had a working pressure of approximately 22 lb/in^2.

The cell density and PA production analysis were carried out by manually sampling the fermentation liquor through a sterile sampling port. Analysis of the dry cell weight per 10 ml of culture with respect to OD_{600} revealed that the relationship between the two parameters was linear, confirming that OD_{600} accurately measured cell density. We measured OD_{600} after diluting the culture with sterile medium to yield an OD_{600} value of less than 0.2.

Protease activity determinations. Protease activity in culture supernatants was determined with resorufin-labeled casein (Boehringer Mannheim Biochemicals, Indianapolis, Ind.). Cultures were grown in baffled shake flasks with shaking at 150 rpm at 37°C until the late log phase or early stationary phase. The cells were removed by sterile filtration of the culture with low-protein-binding 0.22-μm-pore-size cellulose acetate filters (Millipore Corp.). The sterile supernatant was used immediately in the assays, which were performed as described by Twining (45), except that no calcium was added other than the amount present in the medium. Protease activity was measured spectroscopically at 574 nm.

Assay of the M_r 83,000 PA in crude fermentation liquor by SDS-PAGE. Samples for PA determination by sodium dodecyl sulfate-polyacrylamide gel electrophoresis (SDS-PAGE) were filtered through 0.22-μm-pore-size filters and stored at −70°C after the addition of 2 mM EDTA and 20 mM HEPES (pH 7.3). The samples were later concentrated approximately 10-fold with Centricon 30 concentrators (Amicon, Beverly, Mass.) by centrifugation at 4,900 × *g* and were desalted twice by diluting to the original volume with 20 mM HEPES (pH 7.3)–5 mM NaCl–2 mM EDTA and repeating the concentration step. The samples were frozen, lyophilized, dissolved in 50 μl of the HEPES buffer described above, and diluted 1:1 with a twofold-concentrated SDS solubilization buffer consisting of 450 mM Tris-HCl, 4% (wt/vol) SDS, 12% (vol/vol) glycerol, 0.0025% (wt/vol) bromphenol blue, and 0.0025% (wt/vol) phenol red before being heated at 95°C for 5 min. Appropriate dilutions of the solubilized fermentation samples were applied in a total volume of 10 to 15 μl to 10% Tris–Tricine gels (Novex, San Diego, Calif.). The gels were fixed in 10% (vol/vol) acetic acid–50% (vol/vol) methanol (MeOH), stained with 0.05% (wt/vol) Coomassie brilliant blue in 10% (vol/vol) acetic acid for a minimum of 16 h, and destained in 10% (vol/vol) acetic acid. The gels were scanned with a model 420oe optically enhanced, 42-μm-resolution scanner (PDI, Huntington, N.Y.) with QS30 software (PDI). Portions of the gel without protein were randomly chosen and scanned to accurately subtract any background absorption. Standard curves were generated with 100 to 1,000 ng of purified PA on each gel used for the assay. Plots of PA band absorbance against the amount loaded proved linear, with *r* values of 0.992 to 0.996 from linear regression analysis.

Fermentation harvest conditions. At an OD_{600} of 10 to 12, when we noted a pronounced drop in oxygen consumption, the fermentor was cooled to 10°C and EDTA was added to a final concentration of 24 mM. The culture was collected with a peristaltic pump at 25 liters/h through the fermentor harvest valve to a CEPA LE continuous-flow centrifuge (New Brunswick Scientific) equipped with a clarification bowl and centrifuged at 40,000 × *g*. The clarified supernatant was subsequently sterile filtered with a Pellicon cassette system equipped with two 5-ft^2, 0.45-μm-pore-size cellulose acetate cartridges (Millipore Corp).

Purification of PA from fermentor cultures. The sterile supernatant was concentrated with an Amicon DC10L concentrator equipped with two cellulose acetate spiral-wound 30-kDa cutoff cartridges (Amicon) at 5°C from 21 to less than 2 liters at a back pressure of less than 30 lb/in^2. The concentrate was diafiltered at constant retentate volume against 10 volumes of 25 mM diethanolamine 50 mM NaCl–2 mM EDTA–30 mM KCl (pH 8.9). The diafiltered PA was chromatographed at 30 cm/h and 5°C through a 9- by 10-cm packed bed of quaternized amine Macro Prep 50Q resin (Bio-Rad, Hercules, Calif.) in an Vantage-S column (Amicon) previously equilibrated in the same buffer used for the diafiltration. The eluate was concentrated and diafiltered with an S1Y30 30-kDa cutoff cellulose acetate spiral-wound cartridge (Amicon) at an operating pressure of 20 lb/in^2. The final concentrate of ca. 300 ml was diafiltered against 10 volumes of 145 mM ammonium acetate–2 mM EDTA (pH 10.0) and passed through a 0.2-μm-pore-size cellulose acetate filter.

The PA was then applied to an AP-5 (Waters, Milford, Mass.) 5- by 10-cm high-pressure liquid chromatography (HPLC) column at 22 to 23°C with a Waters 650e preparative HPLC apparatus at a linear velocity of 122 cm/h. The column was packed at less than 500 lb/in^2 with bulk 20-μm high-capacity quaternized polyethyleneimine (HQ) resin (Perceptive Biosystems, Cambridge, Mass.) to a bed height of 7.5 cm. A total of 30 mg of protein was loaded per 20 ml of packed resin, and the column was developed with a 10-column-volume linear gradient to 60% of 1.0 M ammonium acetate (pH 10.0)–5% (vol/vol) MeOH. Protein elution was monitored at 280 nm, and EDTA was added to the collected fractions to 2 mM before further analysis by SDS-PAGE. The fractions identified as containing M_r 83,000 PA were then pooled and diluted with sterile MQ water to a final conductivity of 15.5 mS/cm. The pooled fractions were applied to a second AP-5 (Waters) HPLC column packed and run under the same conditions as the HQ column, except that bulk 20-μm quaternized polyethyleneimine (QE) resin (Perceptive Biosystems) was used. A maximum of 1 mg of greater than 80% pure PA was applied per ml of packed-bed volume, which was equilibrated with 85% 50 mM ammonium acetate (pH 10.0)–5% (vol/vol) MeOH and 15% 1 M ammonium acetate (pH 10.0)–5% (vol/vol) MeOH. The column was developed with a 10-column-volume linear gradient to 80% of 1 M ammonium acetate (pH 10.0)–5% (vol/vol) MeOH.

The purified M_r 83,000 PA was pooled and diluted with MQ water to a final conductivity of 12 mS/cm. To maintain the solubility of the dilute protein solution, NaCl was added to a final concentration of 2 mM during the dilution step. The PA was reapplied at 22 to 23°C to the QE column equilibrated with 50 mM ammonium acetate (pH 10.0) and washed with 5 column volumes of the starting buffer. The column was then washed with 50 mM ammonium acetate (pH 8.9) until the eluate pH was equivalent to the buffer pH. Then the PA was eluted with 65% 50 mM ammonium acetate (pH 8.9)–0.5 M NaCl and 35% 50 mM ammonium acetate (pH 8.9). The concentration of the PA was determined by the Bio-Rad protein assay. EDTA was added to 2 mM, and 1-mg aliquots were frozen under liquid nitrogen.

When greater than 90% final purity was required, the PA was applied at 22 to 23°C to an additional ether hydrophobic interaction chromatography (HIC) (Perceptive Biosystems) column. Before application, the PA was equilibrated with 1.75 M ammonium sulfate–100 mM ammonium acetate–2 mM EDTA (pH 10.0) by overnight dialysis against 50 to 100 volumes of buffer. The PA was filtered through 0.22-μm-pore-size low-protein-binding filters and applied to the HIC column at 1.2 mg of PA/ml of HIC resin at a linear flow rate of 1,807 cm/h. The PA was eluted with a linear 10-column-volume gradient from 100% 1.75 M ammonium sulfate–100 mM ammonium acetate (pH 10.0) to 50% 100 mM ammonium acetate (pH 10.0) and 50% 1.75 M ammonium sulfate–100 mM ammonium acetate (pH 10.0). The PA was buffer exchanged into the same storage buffer used for the QE-purified product, frozen under nitrogen, and stored at −70°C.

Analysis of purified M_r 83,000 PA. The purity of the PA was assessed by several different methods. SDS-PAGE was performed as described above, except that the samples were not lyophilized. Native PAGE was performed as recommended by the manufacturer, with 4 to 15% acrylamide Phast gels (Pharmacia Biotech, Piscataway, N.J.).

Reversed-phase HPLC was performed at 22 to 23°C with an R1/M C_4 column (Perceptive Biosystems). The column was equilibrated in 90% solvent A (0.05% [wt/vol] NaOH)–10% solvent B (80% [vol/vol] acetonitrile, 0.05% [wt/vol] NaOH) before injection of 50- to 100-μg samples. The column was developed at a linear flow rate of 1,800 cm/h with a linear 15-column-volume gradient to 80% solvent B. The absorbance at 280 nm (A_{280}) was monitored.

SDS-capillary electrophoresis (CE) was performed with a 270A-HT CE system interfaced with Turbochrom version 4.1 software (Perkin-Elmer Applied Biosystems, Foster City, Calif.) and ProSort SDS-protein analysis reagent (Perkin-Elmer Applied Biosystems) in a 42-cm by 55-μm (inner-diameter) fused-silica capillary. Capillary conditioning and equilibration with ProSort reagent were carried out as described by the manufacturer. PA samples (3 to 4 mg/ml) were diluted 1:1 with 10 mM HEPES (pH 7.3) and then further diluted with SDS–2-mercaptoethanol buffers as suggested by the manufacturer.

Automated N-terminal sequencing was performed on approximately 100 pmol of PA purified by ion-exchange chromatography or by reversed-phase HPLC. All the protein samples were transferred into neutral buffers and further desalted with PD10 desalting columns (Bio-Rad) equilibrated with 5 mM NaCl and 1 mM $CaCl_2$ before being applied to an Applied Biosystems 470A Sequenator (Perkin-Elmer). Phenylthiohydantoin-derived amino acids were identified with a model 120A phenylthiohydantoin analyzer from the same manufacturer. C-terminal sequencing was carried out on polyvinylidene difluoride-adsorbed PA with a Perkin-Elmer Applied Biosystems 477 Sequenator by using the allcylation approach.

The biological activity of purified PA was assessed by an in vitro cytotoxicity test (6). Briefly, various concentrations of PA were combined with 40 ng of LF per ml and added to J774A.1 macrophage monolayers in a volume of 0.1 ml. After 4 h of incubation, 25 μl of (3-[4,5-dimethylthiazol-2-yl]-2,5-diphenyltetrazolium bromide (MTT) (Boehringer Mannheim) at 5 mg/ml was added per well. The cells were lysed after 2 h, and $A_{570} - A_{690}$ was measured. The results were compared with those obtained for PA purified from the Sterne strain by a previously published method (19). The amount of PA required for 50% killing of the cells was determined by linear-regression analysis.

The DNA content of the final purified PA was analyzed with the Hoechst 33258 dye (Polysciences Inc., Warrington, Pa.). Carbohydrate was analyzed by the phenol-sulfuric acid method (3). The results were compared with those obtained after an additional deamination step, as described by Lee and Montgomery (18). No significant difference in the total carbohydrate levels was found, and the phenol-sulfuric acid assay was used without deamination. Because different carbohydrates have different extinction coefficients in this assay (3), the total carbohydrate was determined on a A_{488}/total-volume basis.

Protein samples for immunoblot analysis were separated by SDS-PAGE under reducing conditions on 10% Tris–Tricine gels. Separated proteins were transferred electrophoretically onto 0.2-μm-pore-size nitrocellulose membranes (44) for immunoblotting. The nitrocellulose membranes were blocked with 5% (wt/vol) nonfat dry milk in 10 mM sodium phosphate–0.15 M NaCl (pH 7.3) (PBS-M) before incubation overnight at 4°C with the monoclonal antibody mixture diluted in PBS-M containing 0.05% (vol/vol) Tween 20. The monoclonal antibody mixture consisted of PA2III 2B8, PAI 3B6 PAI 2D5 (21–23), and PA20 15F7 (22), each at a 1:2,000 dilution in PBS-M containing 0.05% (vol/vol) Tween 20. After the membranes were washed with PBS-M–0.05% (vol/vol) Tween 20, they were incubated with a 1:2,000 dilution of horseradish peroxidase-labeled goat anti-mouse immunoglobulin G (Kirkegaard and Perry, Gaithersburg, Md.) for 1 h at room temperature. The membranes were then washed, and the immunoreactive bands were detected either with the enhanced chemiluminescence (ECL) reagent as recommended by the manufacturer (Pierce, Rockford, Ill.) or by adding 4-chloro-1-naphthol and hydrogen peroxide.

RESULTS

Medium effects and growth. The first step in the development of the PA production method was to assess the effects of growth medium on bacterial cell growth, PA production, and protease activity. Good growth rates and high biomass were achieved previously with the ΔSterne-1 strain in a high-tryptone, high-yeast-extract medium (5). When the same medium was investigated with the ΔSterne-1(pPA102)CR4 strain under conditions of low or high aeration in shake flask experiments, the highest cell densities and PA production levels were achieved under aerobic conditions. PA production levels were compared in late-log- to early-stationary-phase aerobic cultures in complete medium (Fig. 1, lane 1), in medium with 25% of the total yeast extract found in complete medium (lane 2), and in medium with 25% of the total tryptone found in complete medium (Fig. 1, lane 3). The largest amount of intact M_r 83,000 PA was observed in complete medium (lane 1), while smaller amounts were generated with the reduced-yeast-extract medium shown in lane 2 and little, if any, intact M_r 83,000 PA was found in the reduced-tryptone medium (lane 3). However, the cell growth in all three media was comparable to the growth in the complete culture (lane 1), reaching 7 OD_{600} units, while the reduced-yeast-extract (lane 2) and reduced-tryptone (lane 3) cultures reached 10 and 8 OD_{600} units, respectively.

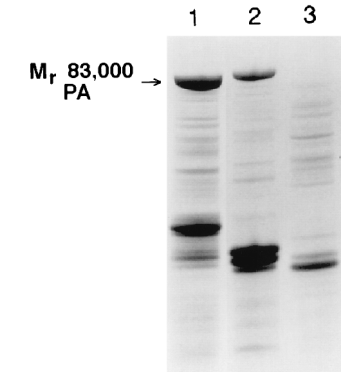

FIG. 1. SDS-PAGE analysis of ΔSterne-1(pPA102)CR4 culture supernatants from complete, reduced-yeast-extract, and reduced-tryptone media. Lanes: 1, complete medium with 33 g of tryptone/liter and 20 g of yeast extract/liter; 2, complete reduced yeast extract medium with 33 g of tryptone/liter and 5 g of yeast extract/liter; 3, complete reduced tryptone medium with 8.25 g of tryptone/liter and 20 g of yeast extract/liter. A 1-ml sample was removed from each culture at late log to early stationary phase. The samples were sterile filtered, buffer exchanged, and concentrated to equivalent volumes. Equivalent volumes were loaded for SDS-PAGE analysis.

We also determined the protease activity in complete medium and 25% tryptone medium culture supernatants by the resorufin-labeled casein assay. Fourfold-higher protease activity was measured for the reduced-tryptone cultures when mid-log-phase cultures of 5 to 6 OD_{600} units were compared (Table 1). The activity in the reduced-tryptone medium increased to as much as 50-fold greater than in complete medium when cultures in stationary phase were compared (data not shown). A second addition of tryptone to the culture supernatants after

TABLE 1. Determination of protease activity in culture supernatants and reduction of measurable activity by tryptone and EDTA

Medium	Additive	Protease activity (mU/OD_{600} unit) (mean ± SD)	% Reduction in measurable activity
Complete	None	15.4 ± 0.6	
Complete	Tryptone	8.3 ± 0.4	46
Complete	EDTA	0.5 ± 0.1	96
1/4 tryptone	None	56.9 ± 2.4	
1/4 tryptone	Tryptone	24.8 ± 1.0	56
1/4 tryptone	EDTA	0.8 ± 0.1	99

[a] Aliquots of each culture were sterile filtered and immediately used for protease assays. Activity was measured by the resorufin-labeled casein assay at 574 nm after a 16-h incubation at 37°C. One unit of activity was defined as one A_{574} unit. The tryptone added was prepared as a 10-fold-concentrated stock (330 g/liter) in MQ water and filtered through a 0.2-μm-pore-size filter to remove insoluble debris. The amount of tryptone added was equivalent to the amount in complete medium (33 g/liter). The final concentration of EDTA (pH 8.0) was 24 mM.

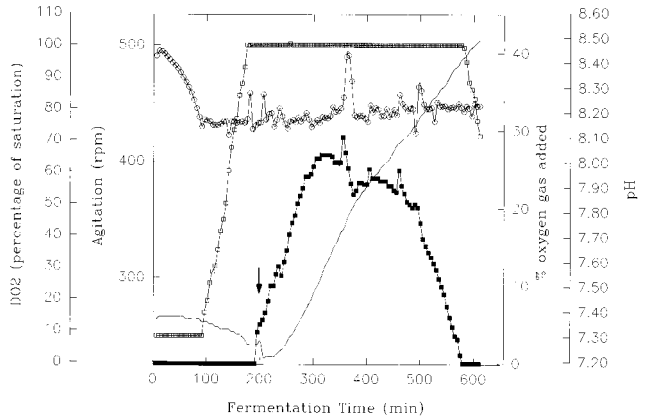

FIG. 2. Physical-chemical parameters from aerobic ΔSterne-1(pPA102)CR4 fermentation. Symbols: open circles, DO_2; solid line, pH; open squares, agitation; solid squares, percent oxygen. The tryptone addition during the fermentation is indicated by the arrow above the percent oxygen data at 200 min. The temperature range was 36.7 to 37.4°C. Pressure was constant at 2.0 lb/in^2, and the sparge rate was 1 vol/vol/min. The sharp positive spike in the DO_2 values at 350 min was due to the addition of antifoam KFO673.

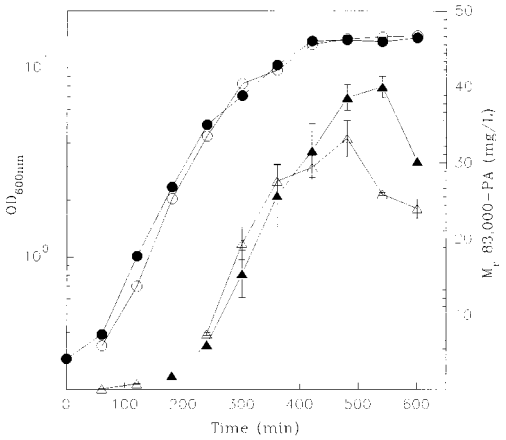

FIG. 3. PA production versus cell density. Symbols: solid circles, growth data 7 July fermentation; open circles, growth data 4 August fermentation; solid triangles, PA yield data 7 July fermentation; open triangles, PA yield data 4 August fermentation. Equivalent volumes were sampled from the 20-liter fermentor for each EFT. The OD_{600} was determined for each EFT, and the samples were sterile filtered. The filtrates were desalted and concentrated to equivalent final volumes before a 1:1 dilution with twofold-concentrated SDS solubilization buffer and analysis by SDS-PAGE. Coomassie blue-stained gels were digitally scanned as described in Materials and Methods, and amounts of M_r 83,000 PA were determined for each EFT.

the bacteria were removed by sterile filtration reduced the measurable effect of the protease on the resorufin-labeled casein in both complete and reduced tryptone medium by 46 and 56%, respectively (Table 1). From the comparable total cell growth in the two media and these protease activity results, the higher levels of tryptone optimized PA production by acting not only as a substrate for growth but also as a surrogate protease substrate, which slowed the proteolytic degradation of PA. Inhibitor studies revealed that the protease activity released into the medium was more than 95% inhibited by the addition of EDTA (Table 1). The combination of the serine protease inhibitor phenylmethylsulfonyl fluoride (PMSF) with EDTA was found to be no more inhibitory than EDTA alone (data not shown). These observations were confirmed by SDS-PAGE analysis of culture supernatants spiked with purified PA (data not shown).

Fermentation. Figure 2 shows the pH, DO_2, percent O_2, and agitation values for a representative fermentation at the 20-liter level. The pH was monitored but not controlled during the course of the fermentation. A small drop in pH can be seen between elapsed fermentation times (EFT) of 50 and 175 min, which we attribute to the production of organic acids from the metabolism of carbohydrates supplied with the yeast extract. After an approximate EFT of 190 to 200 min, the pH began to increase, consistent with the release of ammonium from the aerobic metabolism of amino acids and peptides. After the pH had increased by 0.01 unit, a second addition of tryptone was made as a 10-fold concentrate of the amount added initially to ensure that tryptone never became limiting during the fermentation. Once the tryptone had been added, the pH decreased transiently at 200 to 205 min due to minor temperature and pH differences between the added tryptone and the vessel. The pH increased to a maximum of 8.5 during the course of the fermentation but remained within the acceptable range of 6 to 9 for *B. anthracis* ΔSterne-1(pPA102)CR4 (data not shown).

The DO_2 value dropped from the initial 100% to the set point of 75% at an EFT of ca. 75 min (Fig. 2). The 75% set point was maintained by increasing the agitation from 250 rpm to a maximum of 500 rpm. As shown in Fig. 2, the maximum agitation was reached within 175 min. Since further increases in agitation were counterproductive, due to increased cell shear, supplementing the process air with 100% O_2 gas was necessary because attempts to control the DO_2 by increasing agitation and/or pressure alone failed to maintain a DO_2 value above zero throughout the fermentation. As seen in Fig. 2, oxygen effectively maintained the DO_2 set point once the maximum agitation was achieved. Oxygen supplementation increased steadily throughout the log phase of growth until the deceleration (early stationary) phase was reached at 9 to 12 OD_{600} units and a constant decrease in the percent oxygen occurred. This decrease is seen in Fig. 2 at an EFT of 300 to 325 min. The percentage of oxygen decreased steadily as the cells entered stationary phase, with the exception of a transient rise at 350 min. Once the oxygen supplementation reached zero, the agitation also decreased, suggesting very little demand for oxygen.

The growth curves and yield of M_r 83,000 PA as a function of EFT are shown in Fig. 3 for two representative fermentations. The data demonstrate the reproducibility of the fermentation process and suggest that the maximum cell density under the conditions used is 14 to 15 OD_{600} units. The doubling time was 53.4 ± 3.8 min, and the specific growth rate was 0.0130 ± 0.009 min^{-1}. The growth curves confirmed that the decrease in oxygen consumption at an EFT of 300 to 325 min shown in Fig. 2 occurred during the deceleration (late log to early stationary) phase of growth. The plot of M_r 83,000 PA against EFT also demonstrated that the yield of M_r 83,000 PA also reached a maximum during the deceleration phase of growth. More importantly, it also clearly showed the subsequent decline in product attributable to the protease activity released into the medium by the host strain.

Even though the growth data under nonlimiting aeration proved extremely reproducible, the yield of M_r 83,000 PA was less consistent late in the fermentation (Fig. 3). Based on this yield variability and the rather sudden onset of product loss due to degradation, we selected the decrease in oxygen supplementation seen in Fig. 2 as the main criterion for determining the onset of the deceleration phase and terminating the fermentation. This allowed harvesting at a point near the max-

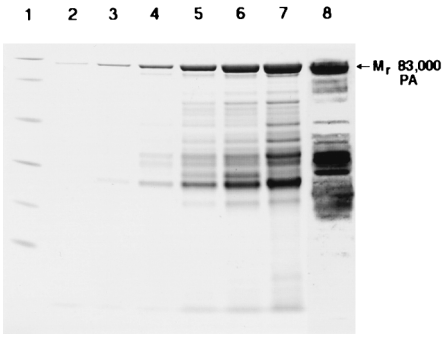

FIG. 4. SDS-PAGE results reflecting the time course of PA production from aerobic fermentation of ΔSterne-1(pPA102)CR4. Lanes: 1, molecular weight standards; 2, EFT 1 h; 3, EFT 2 h; 4, EFT 3 h; 5, EFT 4 h; 6, EFT 5 h; 7, EFT 6 h; 8, immunoblot of EFT 6 h developed with a pool of four monoclonal antibodies. Equivalent sample volumes were taken for each EFT. Samples were sterile filtered, and the filtrate was desalted, lyophilized, and resuspended in buffer to the same final volume before a 1:1 dilution with twofold-concentrated SDS solubilization buffer and analysis by SDS-PAGE. Equal volumes of each sample were applied to the gel. The immunoblot was developed with 4-chloro-1-naphthol after incubation with goat-anti mouse antibody linked to horseradish peroxidase. Bio-Rad low-molecular-weight standards with the following M_rs were used: phosphorylase *b*, 97,400; serum albumin, 66,200; ovalbumin, 45,000; carbonic anhydrase, 31,000; trypsin inhibitor, 21,500; and lysozyme, 14,400.

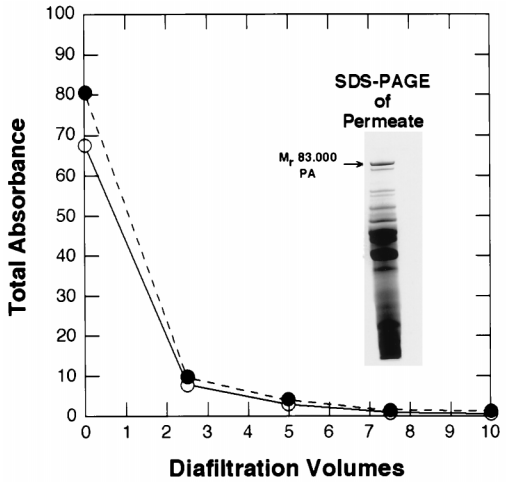

FIG. 5. UV-spectrophotometric and SDS-PAGE analysis of the diafiltration permeate. Symbols: solid circles, A_{260}; open circles, A_{280}. Permeate from the Amicon 30-kDa-cutoff spiral-wound cartridge during the first diafiltration step was collected, diluted with the diafiltration buffer, and analyzed by UV spectroscopy at 280 and 260 nm. The spectrophotometer was blanked against the diafiltration buffer. Values at 350 and 320 nm were measured to confirm that sample turbidity was negligible. The inset shows a Coomassie blue-stained SDS-PAGE gel of a 10-fold concentrate of the diafiltration permeate collected at the outset of the diafiltration step.

imum yield of M_r 83,000 PA yet avoided the ambiguity of terminating the fermentation based on optical density values that were difficult to correlate with the absolute maximum M_r 83,000 PA yield while avoiding excessive product degradation. Even with this selection criterion, the yield from multiple fermentations was found to vary from 20 to 30 mg of M_r 83,000 PA/liter. The steep slope of the plot of M_r 83,000 PA against time seen in Fig. 3 accounted for the relatively wide product yield range.

The results of an SDS-PAGE analysis of concentrated protein samples collected hourly throughout the fermentation are shown in Fig. 4. The constitutive expression of product in precultures and in the vessel resulted in the presence of M_r 83,000 PA at the very first EFT point (lane 2, EFT 1 h). The amount of total protein and M_r 83,000 PA increased with time, up to the decrease in oxygen consumption in the fermentor vessel and point of harvest at an EFT of 5.0 to 5.5 h. The increase in M_r 83,000 PA was accompanied by an increase in the amounts of lower-molecular-weight species, consistent with production accompanied by degradation. An immunoblot of the final EFT sample (lane 8), developed with a mixture of monoclonal anti-PA antibodies (21–23), confirmed that the lower-molecular-weight species in late-log deceleration-phase samples were immunoreactive PA degradation products. At the point of harvest, the total protein yield was 1.2 to 1.6 g, of which 28 to 33% was M_r 83,000 PA.

Purification. The crude fermentation supernatant was sterilized by filtration and then concentrated and diafiltered into ammonium acetate buffer with ultrafiltration spiral-wound cartridges with a molecular mass cutoff of 30 kDa. The diafiltration step was introduced primarily for buffer exchange but was also a critical purification step, as shown by the decrease in total A_{260} and A_{280} in Fig. 5. The decreased UV absorbance reflected the loss of protein, DNA, and RNA. A total diafiltration volume corresponding to 10 times the volume of the protein concentrate was required for the maximum 70- to 80-fold reduction in the UV absorbance seen in Fig. 5. SDS-PAGE analysis of the permeate, shown in the inset in Fig. 5, revealed an enrichment in proteins with M_rs less than 30,000 and little M_r 83,000 PA. Consistent with this, the calculated yield of the product was 90 to 95%. Analysis of the A_{260}/A_{280} ratio for the diafiltered sample containing the product revealed a value of 1.93, which indicates protein that was still contaminated with 69% (by weight) of nucleic acids (8, 26).

The diafiltered protein and nucleic acid mixture was subjected to anion-exchange chromatography with a quaternized-amine resin to remove residual nucleic acid and peptide contaminants. To remove these contaminants without losing the product, we increased the conductivity of the protein mixture to 11 mS/cm with KCl before applying it to the resin. Under these conditions, the PA was not bound by the resin but nucleic acids and other protein contaminants were adsorbed. The A_{260}/A_{280} ratio of the eluted protein was 0.68, which corresponded to a residual nucleic acid content of 1% (8, 26). The total protein recovery was between 50 and 55% of the amount loaded, while the M_r 83,000 PA recovery was 85 to 90%.

Once the nucleic acid contamination was removed, the partially purified protein was diafiltered into ammonium acetate

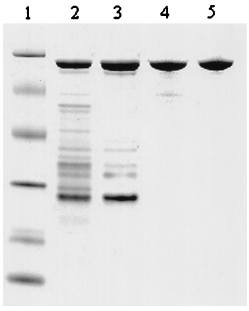

FIG. 6. SDS-PAGE analysis of PA purity after chromatographic purification steps. Lanes: 1, molecular weight standards; 2, PA after Macro-Prep 50 Q chromatography; 3, PA after HQ chromatography; 4, PA after QE chromatography; 5, PA after ether HIC chromatography. PA samples from each purification step were desalted, concentrated, and solubilized in SDS buffer. The total protein loaded in lanes 2 to 5 was 2 μg. Molecular weight standards were as in Fig. 4.

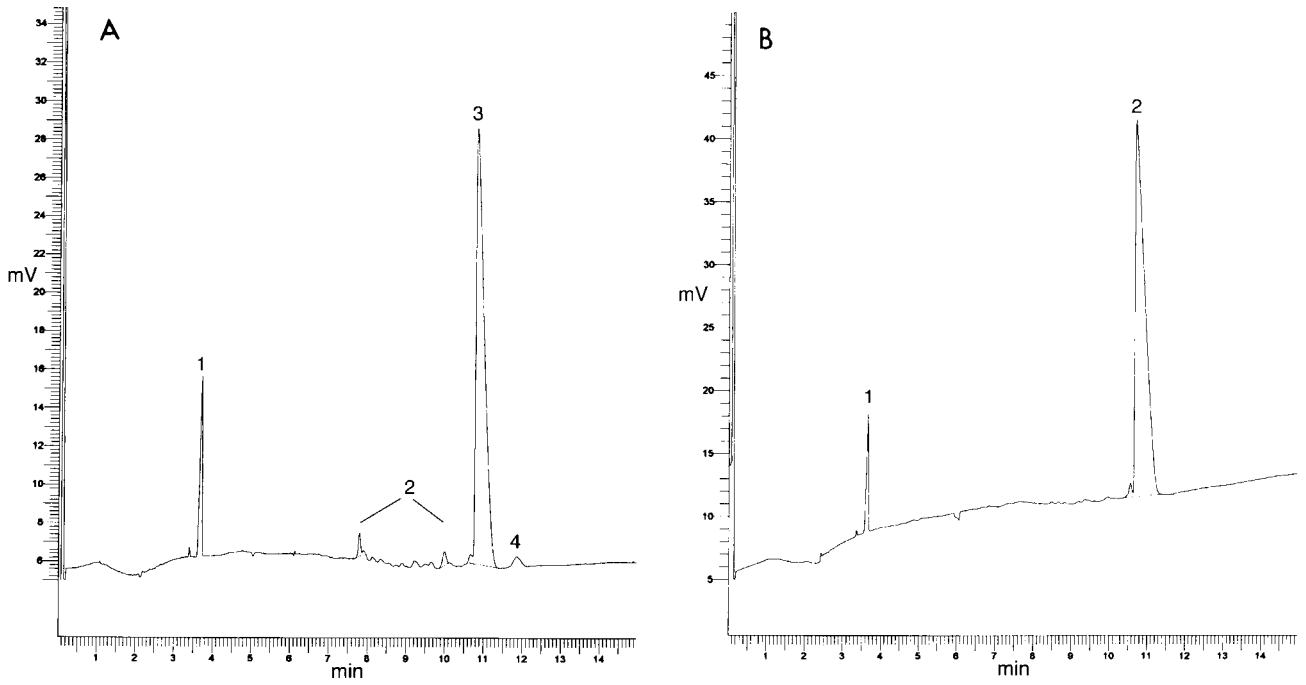

FIG. 7. Determination of PA purity by SDS capillary electrophoresis. PA samples were analyzed after QE (A) or ether HIC (B) chromatography steps. The samples were desalted and concentrated to 3 to 4 mg/ml before being solubilized with SDS as described in Materials and Methods. The samples were applied by electrokinetic injection at −5 kV for 5 to 10 s. Separations were performed at −10 kV for 15 min, and the A_{215} was monitored.

buffer (pH 10) and concentrated approximately fourfold with a spiral-wound 30-kDa cutoff ultrafiltration membrane. The starting material for the HQ anion-exchange quaternized polyethyleneimine HPLC column is shown in Fig. 6, lane 2. The substantial purification achieved before HPLC chromatographic steps can be seen by comparing Fig. 6, lane 2, with Fig. 4, lane 7.

The partially purified material was applied to an HPLC HQ quaternized-amine ion-exchange column and eluted with a 10-column-volume linear ammonium acetate gradient. The M_r 83,000 PA was resolved from the majority of the contaminating polypeptides that failed to adsorb under these conditions and from two other peaks, which eluted before and after PA. The approximately 50 to 60% pure PA (Fig. 6, lane 3) was then diluted to 15 mS/cm with MQ water and applied to a QE quaternized-polyethyleneimine perfusion anion-exchange resin with a lower charge density and different selectivity than the HQ resin. At this pH, a single asymmetric peak was eluted with a 10-column-volume linear ammonium acetate gradient. The M_r 83,000 PA eluted at the front end, while the major impurities eluted later in the gradient as a pronounced shoulder. This fractionation of the main peak resulted in recovery of 35 to 40% of the initial M_r 83,000 PA present in the fermentor and a product that was typically 88 to 93% pure (lane 4).

Although the QE-purified M_r 83,000 PA fulfilled the initial goal of greater than 85% purity, we later determined that higher purity could be achieved by HIC, an orthogonally related chromatographic separation technique with separation based on hydrophobicity. The method was developed by using an ether-based HIC resin and a pH 10 buffer composed of ammonium sulfate and ammonium acetate. Under these initial buffer conditions, the M_r 83,000 PA bound to the column at 22 to 23°C while the remaining impurities eluted with an isocratic wash. The M_r 83,000 PA (Fig. 6, lane 5) was eluted with a linear gradient, although step gradient elution was also possible. The recovery of M_r 83,000 PA from this step was 90%, and the final purity was 95 to 98%. Although there was a previous report of an HIC method for PA, it proved difficult to compare the techniques because the temperature range and recovery for the previously reported method were not defined (38). In our hands, the ether HIC proved superior in final product purity and recovery to that of the previous report.

Analysis of product purity. The final product purity described above was determined by SDS-CE and reversed-phase chromatography. Figure 7A shows the SDS-CE analysis of QE-purified recombinant PA monitored at 215 nm. The main M_r 83,000 PA peak at 10.8 min is labeled 3, while the other major peak, labeled 1, at 3.65 min is the mellitic acid internal standard. The impurities can be seen as multiple single and double peaks collectively labeled 2 between 7.5 and 10.5 min. The peak labeled 4 at 11.99 min was investigated further and found to be identical to a contaminant with an M_r of 80,000 by SDS-PAGE. The reason for the increased estimated mass relative to the M_r 83,000 PA with SDS-CE was not clear, but the observed baseline resolution of SDS-CE made an assay of this 1 to 3% contaminant possible. Overall integration of the peak area of the M_r 83,000 PA and the sum of all the contaminants yielded a final PA purity of 90% for this lot. Analysis of the same PA after HIC purification (Fig. 7B) revealed a final purity of 98% with trace contaminants between 8 and 10.5 min at the threshold of detection. The only significant resolved contaminant peak was seen as a shoulder of the PA peak at 10.6 min, which was believed to be a minor related impurity that was also visualized as a slightly faster-migrating minor band by SDS-PAGE and immunoblotting (data not shown). The HIC step was extremely effective in removing the contaminant labeled 4 in Fig. 7A. The results shown in Fig. 7A and B also indicated that neither sample contained detectable peptide contamination since such impurities eluted after the internal standard in the 4- to 7-min range (data not shown).

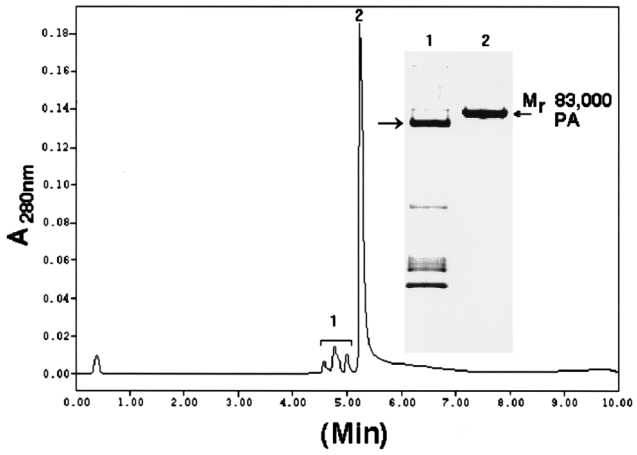

FIG. 8. Reversed-phase HPLC analysis of PA. A 100-μg sample of POROS QE-purified PA was subjected to reversed-phase HPLC analysis. The three main absorbance peaks labeled 1 were collected and pooled, and peak 2 was collected separately. Fractions collected for SDS-PAGE were immediately neutralized by adding 20 mM HEPES (pH 7.3) and diluting 1:1 with MQ water before concentrating. The results of Coomassie blue-stained SDS-PAGE are shown in the inset. The numbering of the inset lanes corresponds to the peak labeling. The M_r 80,000 contaminant in lane 1 is identified by an arrow to the left of the inset.

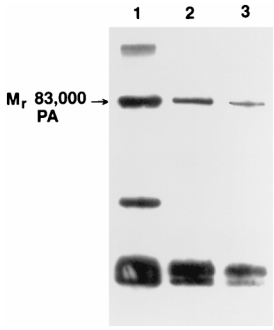

FIG. 9. Immunoblot analysis of the total impurities in M_r 83,000 PA purified by QE anion-exchange chromatography. The pooled protein contaminants from three separate lots of PA were purified by reversed-phase HPLC, separated by SDS-PAGE, and transferred electrophoretically to nitrocellulose membranes. The immunoreactive bands were detected with the ECL reagent and a pool of monoclonal antibodies as described in Materials and Methods.

Purified PA was also analyzed by reversed-phase chromatography. PA lost solubility in the presence of acidic reversed-phase ion-pairing agents, necessitating the development of an alkaline reversed-phase method. The reversed-phase separation of QE-purified PA with 0.05% (wt/vol) NaOH as the ion-pairing agent is shown in Fig. 8. Integrating the detected peaks yielded an identical estimate of 90% purity for the same lot of QE-purified PA analyzed by SDS-CE in Fig. 7A. The small peak at the beginning of the chromatogram is due to added EDTA and was not included in the total integrated peak area. The series of three peaks collectively labeled 1 and the main peak, labeled 2, were collected, concentrated, and further analyzed by SDS-PAGE. The polypeptides were collected into sufficient HEPES (pH 7.3) to avoid prolonged exposure and breakdown of the peptide backbone under the alkaline conditions. The results of the SDS-PAGE analysis are shown as the inset in Fig. 8. After concentration, the pooled multiple peaks (peak 1) contained six major polypeptide contaminants (lane 1 of inset) while peak 2 contained the M_r 83,000 PA (lane 2 of inset). Although the resolution value of the M_r 83,000 PA from the nearest contaminant peak was greater than 2.1, some M_r 83,000 PA coeluted with peak 1. The reason for this remains unclear, but it is possible that this PA was partially denatured. Significantly, reapplication of M_r 83,000 PA in peak 2 to the reversed-phase column resulted in a single peak with a retention time identical to that of the initial peak 2, making it unlikely that the reversed-phase method caused the changes resulting in the earlier elution pattern. Reversed-phase analysis of the same lot of HIC-purified PA shown in Fig. 7B revealed the same 98% purity level found by SDS-CE (data not shown).

Several different lots of purified PA were subjected to this reversed-phase separation to determine the presence of related and unrelated impurities after the QE stage of the purification. Figure 9 shows an immunoblot of the pooled protein contaminants in peak 1 from three separate lots. The immunoblot was probed with a mixture of four monoclonal antibodies, which had been mapped to different domains of PA (21–23) and visualized with the ECL system. The immunoreactivity of the polypeptides in Fig. 9 confirmed that 7 to 9% of the total impurities remaining in the QE-purified PA that were separated by reversed-phase chromatography were related impurities. The percentage of related impurities and distribution remained constant in stability studies, suggesting that protease activity was removed from the M_r 83,000 PA during purification (data not shown).

The higher-molecular-weight immunoreactive species was M_r 83,000 PA, while the major M_r 80,000 protein contaminant seen in Fig. 8 (inset lane 1) was not immunoreactive. This suggested that the M_r 80,000 contaminant which was present at 1 to 3% in the QE-purified PA was an unrelated impurity. The M_r 80,000 protein was purified by reversed-phase chromatography and subjected to N-terminal sequencing. The N-terminal sequence was determined to be N-ETLKE . . . C, while the M_r 83,000 PA isolated in the same manner yielded an N-terminal sequence of N-EVKQEN . . . C, which corresponded exactly to the DNA-derived amino acid sequence of PA. The sequence of the M_r 80,000 impurity did not correspond to the plasmid-encoded neomycin resistance gene product (28) or to any known *B. anthracis* proteins. The identity of the unrelated impurity remains unknown, since a search of the current protein data banks revealed no significant homologies.

Native PAGE of purified recombinant PA revealed the presence of microheterogeneity in the final product in the form of three major isoforms that were visualized as separate bands (data not shown). The presence of these isoforms was described previously for PA purified from the attenuated *B. anthracis* Sterne strain (20). Comparing the recombinant PA with PA from the Sterne strain revealed the same isoforms in both, although the recombinant was enriched in the upper three of the five total isoforms (data not shown). To determine whether the isoforms were the result of N- or C-terminal proteolysis, the recombinant PA that had three isoforms was subjected to both N- and C-terminal sequencing. The sequence data from the N terminus were N-EVKQEN . . . C, while the C terminus was N- . . . . . FSSKKGYEIG-C. Data from both termini yielded single conclusive sequences that correlated exactly with the DNA-derived amino acid sequences.

The biological activity of the recombinant PA was monitored by the macrophage lysis assay (6) against PA purified by the original protocol from the Sterne strain as a control (19). The cytotoxicity assay was performed by titrating the amount of PA added to the J774A.1 cells with 40 ng of LF per ml and measuring the cell viability. The titration curve generated with the control Sterne PA was comparable to that generated with multiple lots of the purified recombinant PA (data not shown).

The amount of Sterne or recombinant PA required to kill 50% of the cells was 8 to 9 and 3 to 5 ng/ml, respectively. Because the curves and 50% control values were comparable for PA from both sources, the biological activity was clearly not adversely affected by the production or purification methods described here.

DISCUSSION

The major rationale for the continued use of a *B. anthracis* expression system was the direct secretion and accumulation of the desired protein into culture medium in a relatively pure state. In addition, the secretion apparatus was the native secretion system for PA, ensuring that the secreted protein would have the signal sequence correctly removed and that the protein would be correctly folded. An additional rationale for selecting the *B. anthracis* strain was the observed low protease activity in culture supernatants. The greater than 95% inhibition of supernatant protease activity by EDTA and the low (less than 30%) inhibition by PMSF alone made it unlikely that *B. anthracis* excreted significant subtilisin or related alkaline protease activity under the conditions used here. In addition, the lack of additional inhibition when PMSF, benzamidine, or 4-(2-aminoethyl)-benzenesulfonyl fluoride hydrochloride (AEBSF) was added in addition to EDTA suggested the presence of fewer proteases under the growth conditions and medium used here than observed for other bacilli such as *B. subtilis* (1, 34). The inhibition of EDTA was consistent with a neutral or metalloprotease(s) (16, 27), although the presence of a calcium-dependent, serine-type protease (2, 34), as described for *B. subtilis*, could not be ruled out. The plausibility of omitting PMSF from the entire process was confirmed when no loss of product, increase in related impurities, or decrease in stability upon storage at 4°C was observed when only EDTA was added. The lack of a PMSF requirement was a key factor in the selection of *B. anthracis* as a host over *B. subtilis*, since the addition of this toxic inhibitor was essential for stable PA when it was isolated from *B. subtilis* strains. This included the recombinant strain *B. subtilis* WB600, which had six unique protease genes deleted but still required PMSF addition to inhibit its remaining activity (50).

Fermentation of the asporogenic variant ΔSterne-1(pPA102) CR4 under the conditions described here resulted in no detectable spore production and had the secondary effect of greatly reducing the amounts of surface array protein normally released into the supernatant under the conditions used here (5). The reduction in the amount of the surface array protein was not investigated further but was attributed to pleiotropic effects of the spontaneous mutation selected on Congo Red or to a second, uncharacterized mutation.

Comparison of growth in complete medium, reduced yeast extract, or reduced tryptone revealed no change in cell density or growth rate, suggesting that the observed decrease in oxygen use observed at approximately 10 to 12 OD_{600} units in complete medium was not attributable to substrate limitation. Attempts at medium supplementation at this point did not increase overall cell densities or eliminate the drop in oxygen consumption. These observations were most consistent with the accumulation of a toxic metabolic by-product rather than the shortage of a critical nutrient as the cause of the observed cessation of growth. Because the aerobic fermentation of amino acids and peptides increases culture pH due to released ammonium, the ammonium levels (47) generated during fermentation were determined (data not shown). The final concentration of ammonium found during the fermentations and a twofold-higher concentration were tested as potential growth inhibitors by adding ammonium sulfate to aerobic shake flask cultures. Neither concentration had any effect on growth, suggesting that the accumulation of ammonium was not the reason for the cessation of growth under the fermentation conditions described here.

Although maintaining the high DO_2 set point of 75% optimized the growth rate, it may also have led to the observed limitation in cell density by facilitating the rapid accumulation of metabolic by-products. However, the susceptibility of PA to proteolytic degradation even in the presence of tryptone necessitated the development of a rapid fermentation process. The rationale for optimizing growth rates can be seen from the M_r 83,000 PA yield data. Clearly, the yield of M_r 83,000 PA reached a peak during the deceleration (early stationary) phase and then declined rapidly. This decline in the M_r 83,000 PA level directly reduced yield and complicated the purification of M_r 83,000 PA from the increasingly complex mixture of proteolytic degradation products.

Our results demonstrated that tryptone was essential for reducing the measured protease activity and maximizing product recovery at the end of the fermentation. SDS-CE analysis of filtered, nondialyzed tryptone revealed the presence of multiple species, with the majority of the material having a mass less than 15 kDa with minor contributions of higher-mass species. The addition of completely hydrolyzed protein in the form of Casamino Acids was ineffective in protecting PA from proteolytic degradation. These results suggest that it was the polypeptides in tryptone that were crucial to the observed effects on blocking of protease activity. It remains unclear whether the proteolysis is blocked by polypeptides interacting with the protease active site(s) or whether tryptone contributes to a reduction in the actual amounts of protease released into the medium by this organism.

The combination of diafiltration and the initial ion-exchange chromatography resulted in the removal of more than 99% of the nucleic acids and 70% of the carbohydrates. These steps also contributed significantly to the overall purification by eliminating up to 50% of the contaminating protein in the crude fermentation liquor while M_r 83,000 PA recoveries were consistently around 90%. The subsequent ion-exchange purification yielded a product with 88 to 93% purity. The major losses in the whole process occurred during the second of these column purifications, with recoveries of 30 to 40% of the total initial product. These losses were incurred in part because of microheterogeneity in PA, which is readily observed in the form of multiple discrete bands or isoforms by native PAGE (19). The isoforms with higher mobility on native gels coeluted with lower-M_r proteins, reducing the yield, while additional losses were incurred due to coelution of the M_r 80,000 nonrelated impurity with the isoforms of lower mobility. The net result was a loss of 40 to 50% of the PA recovered from the HQ ion-exchange step and a product enriched in three of the initial isoforms.

The alkaline pH used during the purification was chosen for three reasons: (i) to avoid the pH optimum for the remaining contaminating protease(s), (ii) to maintain a sufficient difference from the pI of PA to minimize charge differences between isoforms, and (iii) to minimize protein-protein interactions between intact PA and proteolytic degradation products. The alkaline buffers were instituted with caution since biological activity was a criterion for final product and since exposure of PA to alkaline pH values greater than 8.9 to 9.0 was not previously reported. Comparing the biological activity of samples of PA purified under the conditions described here with PA purified under more physiological pH conditions revealed equivalent activities in the macrophage lysis assay. The data

suggest that the exposure to alkaline conditions did not affect the native folding state of PA, or did so in a manner that was not apparent in the cell lysis assay. We also compared the isoform content to that of PA purified under physiological pH conditions, since prolonged exposure of proteins to alkaline pH can drive the nonenzymatic deamination of asparagine residues to aspartate and isoaspartate residues (33). No shift in the isoform content or in the relative proportions of the isoforms was observed after exposure to buffers used here.

We also investigated the HIC method as a substitute for QE chromatography. The M_r 83,000 PA was purified from the multiple small contaminants with excellent yield, but the product was simultaneously enriched with M_r 37,000 and M_r 47,000 proteolytic fragments of PA that did not dissociate under nondenaturing conditions (32). The copurification of the proteolytically cut species of PA indicated that the HIC method was most useful as a final step.

Clearly, the investigation reported here was undertaken to improve on the undesirable aspects of the current vaccine production system. The production process described here successfully met a number of those goals, including production from an avirulent, asporogenic, nontoxigenic strain; fermentation in the absence of added antibiotic; and minimization of product proteolysis without the addition of the toxic protease inhibitor PMSF. In addition, we designed a 4-day purification process which is robust and flexible enough to overcome potential changes in the amount and ratio of impurities in the starting material yet produces the desired product in adequate yield and desired purity at the desired scale. The purities given were defined on the basis of new and orthogonally related SDS-CE and reversed-phase methods that agreed within 1 to 2% of each other. Finally, immunization studies carried out with PA produced by ΔSterne-1(pPA102)CR4 and purified by the methods described here have proved comparable in efficacy to studies with the current licensed vaccine as a control (12, 14, 35).

ACKNOWLEDGMENTS

We thank Jim Schmidt and Meri Bozzini for their expert sequencing work and Pat Worsham for the asporogenic strain used here. We also acknowledge Arthur M. Friedlander and George Anderson for their support, helpful discussion, and careful but prompt review of the manuscript.

REFERENCES

1. **Arbigen, M. V., B. A. Bulthuis, J. Schultz, and D. Crabb.** 1993. Fermentation of *Bacillus*, p. 871–895. *In* A. L. Sonenshein, J. A. Hoch, and R. Losick (ed.), *Bacillus subtilis* and other gram-positive bacteria. American Society for Microbiology, Washington, D.C.
2. **Bruecker, R., O. Shoseyov, and R. H. Doi.** 1990. Multiple active forms of a novel serine protease from *Bacillus subtilis*. Mol. Gen. Genet. **221:**486–490.
3. **Dubois, M., K. A. Gilles, T. K. Hamilton, P. A. Rebers, and F. Smith.** 1956. Colorimetric method for determination of sugars and related substances. Anal. Chem. **28:**350–353.
4. **Ezzell, J. W., and T. G. Abshire.** 1992. Serum protease cleavage of *Bacillus anthracis* protective antigen. J. Gen. Microbiol. **138:**543–549.
5. **Farchaus, W., W. J. Ribot, M. B. Downs, and J. W. Ezzell.** 1995. Purification and characterization of the major surface array protein from the avirulent *Bacillus anthracis* strain Delta Sterne-1. J. Bacteriol. **177:**2481–2489.
6. **Friedlander, A. M.** 1986. Macrophages are sensitive to anthrax lethal toxin through an acid-dependent process. J. Biol. Chem. **261:**7123–7126.
7. **Friedlander, A. M., S. L. Welkos, M. L. M. Pitt, J. W. Ezzell, P. L. Worsham, K. J. Rose, B. E. Ivins, J. R. Lowe, G. B. Howe, P. Mikesell, and W. B. Lawrence.** 1993. Postexposure prophylaxis against experimental inhalation anthrax. J. Infect. Dis. **167:**1239–1242.
8. **Glasel, J. A.** 1995. Validity of nucleic acid purities monitored by 260nm/280nm absorbance ratios. BioTechniques **19:**62–63.
9. **Gordon, V. M., K. R. Klimper, N. Arora, M. A. Henderson, and S. H. Leppla.** 1995. Proteolytic activation of bacterial toxins by eukaryotic cells is performed by furin and additional cellular proteases. Infect. Immun. **63:**82–87.
10. **Green, B. D., L. Battisti, T. M. Koehler, C. B. Thorne, and B. E. Ivins.** 1985. Demonstration of a capsule plasmid in *Bacillus anthracis*. Infect. Immun. **49:**291–297.
11. **Ivins, B. E., J. W. Ezzell, J. Jemski, K. W. Hedlund, J. D. Ristroph, and S. H. Leppla.** 1986. Immunization studies with attenuated strains of *Bacillus anthracis*. Infect. Immun. **52:**454–458.
12. **Ivins, B. E., J. W. Farchaus, J. Novak, M. L. Pitt, P. F. Fellows, W. J. Ribot, M. P. Stein, and S. Byrd.** 1994. Vaccine efficacy of *Bacillus anthracis* protective antigen produced in prokaryotic and eukaryotic cells, abstr. E-38, p. 150. *In* Abstracts of the 94th General Meeting of the American Society for Microbiology 1994. American Society for Microbiology, Washington, D.C.
13. **Ivins, B. E., P. F. Fellows, and G. O. Nelson.** 1994. Efficacy of a standard human anthrax vaccine against *Bacillus anthracis* spore challenge in guinea pigs. Vaccine **12:**872–874.
14. **Ivins, B. E., P. F. Fellows, L. Pitt, J. Estep, J. Farchaus, A. Friedlander, and P. Gibbs.** 1995. Experimental anthrax vaccines: efficacy of adjuvants combined with protective antigen against an aerosol *Bacillus anthracis* spore challenge in guinea pigs. Vaccine **13:**1779–1784.
15. **Ivins, B. E., and S. L. Welkos.** 1986. Cloning and expression of the *Bacillus anthracis* protective antigen in *Bacillus subtilis*. Infect. Immun. **54:**537–542.
16. **Keay, L.** 1969. Neutral proteases of the genus *Bacillus*. Biochem. Biophys. Res. Commun. **36:**257–265.
17. **Klimpel, K. R., S. S. Molloy, G. Thomas, and S. H. Leppla.** 1992. Anthrax toxin protective antigen is activated by a cell surface protease with the sequence specificity and catalytic properties of furin. Proc. Natl. Acad. Sci. USA **89:**10277–10281.
18. **Lee, Y. C., and R. Montgomery.** 1960. Determination of hexosamines. Arch. Biochem. Biophys. **93:**292–296.
19. **Leppla, S. H.** 1988. Production and purification of anthrax toxin. Methods Enzymol. **165:**103–116.
20. **Leppla, S. H.** 1991. The anthrax toxin complex, p. 277–302. *In* J. E. Alouf and J. H. Freer (ed.), Sourcebook of bacterial toxins. Academic Press, Inc., San Diego, Calif.
21. **Little, S., S. H. Leppla, and E. Cora.** 1988. Production and characterization of monoclonal antibodies to the protective antigen component of *Bacillus anthracis* toxin. Infect. Immun. **56:**1807–1813.
22. **Little, S. F.** 1997. Unpublished data.
23. **Little, S. F., J. M. Novak, J. R. Lowe, S. H. Leppla, Y. Singh, K. R. Klimpel, B. C. Lidgerding, and A. M. Friedlander.** 1996. Characterization of lethal factor binding and cell receptor binding domains of protective antigen of *Bacillus anthracis* using monoclonal antibodies. Microbiology **142:**707–715.
24. **Makino, S., C. Sasakawa, I. Uchida, N. Terakado, and M. Yoshikawa.** 1988. Cloning and CO_2-dependent expression of the genetic region for encapsulation from *Bacillus anthracis*. Mol. Microbiol. **2:**371–376.
25. **Makino, S. I., I. Uchida, N. Terakado, C. Sasakawa, and M. Yoshikawa.** 1989. Molecular characterization and protein analysis of the *cap* region, which is essential for encapsulation in *Bacillus anthracis*. J. Bacteriol. **171:**722–730.
26. **Manchester, K. L.** 1995. Value of A260/A280 ratios of measurement of purity of nucleic acids. BioTechniques **19:**208–210.
27. **McConn, J. D., D. Tsuru, and K. T. Yasunobu.** 1964. *Bacillus subtilis* neutral proteinase. J. Biol. Chem. **239:**3706–3715.
28. **McKenzie, T., T. Hoshino, T. Tanaka, and N. Sueoka.** 1986. The nucleotide sequence of pUB110: some salient features in relation to replication and its regulation. Plasmid **15:**93–103.
29. **Mikesell, P., B. E. Ivins, J. D. Ristroph, and T. M. Dreier.** 1983. Evidence for plasmid-mediated toxin production in *Bacillus anthracis*. Infect. Immun. **39:**371–376.
30. **Mock, M., E. LaBruyere, P. Glaser, A. Danchin, and A. Ullman.** 1988. Cloning and expression of the calmodulin-sensitive *Bacillus anthracis* adenylate cyclase in *Escherichia coli*. Gene **64:**277–284.
31. **Novak, J., J. W. Ezzell, and A. M. Friedlander.** 1996. Personal communication.
32. **Novak, J. M., M. P. Stein, S. F. Little, S. H. Leppla, and A. M. Friedlander.** 1992. Functional characterization of protease-treated *Bacillus anthracis* protective antigen. J. Biol. Chem. **267:**17186–17193.
33. **Paranandi, M. V., A. W. Guzzetta, W. S. Hancock, and D. W. Aswad.** 1994. Deamidation and isoaspartate formation during in vitro aging of recombinant tissue plasminogen activator. J. Biol. Chem. **269:**243–253.
34. **Pero, J., and A. Sloma.** 1993. Proteases, p. 939–952. *In* A. L. Sonenshein, J. A. Hoch, and R. Losick (ed.), *Bacillus subtilis* and other gram-positive bacteria. American Society for Microbiology, Washington, D.C.
35. **Pitt, M. L. M., B. E. Ivins, J. E. Estep, J. Farchaus, and A. M. Friedlander.** 1996. Comparison of the efficacy of purified protective antigen and MDPH to protect nonhuman primates from inhalation anthrax, p. 130. *In* P. C. Turnbull (ed.), Proceedings of the International Workshop on Anthrax, 19–21 September 1995, Winchester, England. Salisbury Medical Bulletin (no. 87, special supplement). Salisbury Medical Society, Salisbury, England.
36. **Puziss, M., L. C. Manning, L. W. Lynch, E. Barclay, I. Abelow, and G. G. Wright.** 1963. Large-scale production of protective antigen of *Bacillus anthracis* anaerobic cultures. Appl. Microbiol. **11:**330–334.
37. **Puziss, M., and G. G. Wright.** 1962. Studies on immunity in anthrax. X.

Gel-adsorbed protective antigen for immunization of man. J. Bacteriol. **85:** 230–236.
38. **Quinn, C. P., C. C. Shone, P. C. B. Turnbull, and J. Melling.** 1988. Purification of anthrax-toxin components by high-performance anion-exchange, gel-filtration and hydrophobic-interaction chromatography. Biochem. J. **252:** 753–758.
39. **Ristroph, J. D., and B. E. Ivins.** 1983. Elaboration of *Bacillus anthracis* antigens in a new, defined culture medium. Infect. Immun. **39:**483–486.
40. **Robertston, D. L., and S. H. Leppla.** 1986. Molecular cloning and expression in *Escherichia coli* of the lethal factor gene of *Bacillus anthracis*. Gene **44:**71–78.
41. **Robertson, D. L., M. T. Tippetts, and S. H. Leppla.** 1988. Nucleotide sequence of the *Bacillus anthracis* edema factor gene (*cya*): a calmodulin-dependent adenylate cyclase. Gene **73:**363–371.
42. **Sirard, J. C., M. Mock, and A. Fouet.** 1994. The three *Bacillus anthracis* toxin genes are coordinately regulated by bicarbonate and temperature. J. Bacteriol. **176:**5188–5192.
43. **Thorne, C. B.** 1985. Genetics of *Bacillus anthracis*, p. 56–62. *In* L. Leive, P. F. Bonventre, J. A. Morello, S. Schlesinger, S. D. Silver, and H. C. Wu (ed.), Microbiology—1985. American Society for Microbiology, Washington, D.C.
44. **Towbin, H., T. Staehelin, and J. Gordon.** 1979. Electrophoretic transfer of proteins from polyacrylamide gels to nitrocellulose sheets: procedure and some applications. Proc. Natl. Acad. Sci. USA **76:**4350–4354.
45. **Twining, S. S.** 1984. Fluorescein isothiocyanate-labeled casein assay for proteolytic enzymes. Anal. Biochem. **143:**30–34.
46. **Uchida, I., T. Sekizaki, K. Hashimoto, and N. Terakado.** 1985. Association of the encapsulation of *Bacillus anthracis* with a 60-megadalton plasmid. J. Gen. Microbiol. **137:**363–367.
47. **Weatherburn, M. W.** 1957. Phenol-hypochlorite reaction for determination of ammonia. Anal. Chem. **39:**971–974.
48. **Welkos, S. L., J. R. Lowe, F. Eden-McCutchen, M. Vodkin, S. H. Leppla, and J. J. Schmidt.** 1988. Sequence and analysis of the DNA encoding protective antigen of *Bacillus anthracis*. Gene **69:**287–300.
49. **Worsham, P. L., and M. R. Sowers.** Isolation of an asporogenic (*spo0A*) protective antigen-producing strain of *Bacillus anthracis*. Submitted for publication.
50. **Wu, X. C., W. Lee, L. Tran, and S. L. Wang.** 1991. Engineering a *Bacillus subtilis* expression-secretion system with a strain deficient in six extracellular proteases. J. Bacteriol. **173:**4952–4958.